

Copyright

By

Abdolhamid Hadibeik Nishaboori

2009

**WIRELINE AND WHILE-DRILLING FORMATION-TESTER
SAMPLING WITH OVAL, FOCUSED, AND CONVENTIONAL
PROBE TYPES IN THE PRESENCE OF WATER- AND OIL-BASE
MUD-FILTRATE INVASION IN DEVIATED WELLS**

by

ABDOLHAMID HADIBEIK NISHABOORI, B.Sc.

THESIS

Presented to the Faculty of the Graduate School of

The University of Texas at Austin

in Partial Fulfillment

of the Requirements

for the Degree of

MASTER OF SCIENCE IN ENGINEERING

The University of Texas at Austin

December 2009

The Thesis Committee for Abdolhamid Hadibeik Nishaboori
certifies that this is the approved version of the following thesis:

**WIRELINE AND WHILE-DRILLING FORMATION-TESTER
SAMPLING WITH OVAL, FOCUSED, AND CONVENTIONAL
PROBE TYPES IN THE PRESENCE OF WATER- AND OIL-BASE
MUD-FILTRATE INVASION IN DEVIATED WELLS**

Committee:

Carlos Torres-Verdín, Supervisor

Kamy Sepehrnoori, Co-Supervisor

Acknowledgements

The author wishes to thank Dr. Carlos Torres-Verdín for providing me the opportunity to work with him, the valuable time, and effort dedicated to educate and prompt my knowledge with his supervision. I would also like to thank Dr. Kamy Sepehrnoori for all his guidance and efforts as my co-supervisor. My gratitude to the mentioned professors is endless and memorable.

I would also like to thank the faculty and staff of Petroleum and Geosystems Engineering Department, specially Dr. Larry Lake, Dr. Russell Johns, and Dr. Maghsood Abbaszadeh for their help. I am also thankful to Dr. Roger Terzian, Cheryl Kruzic, and Reynaldo Casanova for their help and guidance.

I would also like to thank my colleagues and friends Renzo Angeles, Meghdad Roshanfekar, Gholamreza Garmeh, Mayank Malik, Kaveh Ahmadi, Ali Moinfar, Amirreza Rahmani, Jorge Sanchez, Robert Mallan, Dr. David Wolf, Rohollah Abdolahpour, Waleed Fazelipour, Javad Behseresht, Vahid Shabro, and Siyavash Motealleh. Special gratitude goes to Mark Proett, Mike Bittar, and Bob Engelman (Halliburton Energy Services) for their technical support.

The work described in this thesis was funded by The University of Texas at Austin Research Consortium on Formation Evaluation, jointly sponsored by Anadarko, Aramco, Baker-Hughes, BG, BHP Billiton, BP, Chevron, ConocoPhillips, ENI,

ExxonMobil, Halliburton, Hess, Marathon, Mexican Institute for Petroleum, Nexen, Petrobras, RWE, Schlumberger, StatoilHydro, TOTAL, and Weatherford.

**WIRELINE AND WHILE-DRILLING FORMATION-TESTER
SAMPLING WITH OVAL, FOCUSED, AND CONVENTIONAL
PROBE TYPES IN THE PRESENCE OF WATER- AND OIL-BASE
MUD-FILTRATE INVASION IN DEVIATED WELLS**

Abdolhamid Hadibeik Nishaboori, M.S.E.

The University of Texas at Austin, 2009

Supervisor: Dr. Carlos Torres-Verdín

Co-supervisor: Dr. Kamy Sepehrnoori

Speculation about the potential of developing new fluid sampling methods with probe-type formation testers has existed since the introduction of formation pressure testing to the drilling environment in 2002. Extending the existing wireline technology requires a new pumping system capable of removing invasion fluids and then filling single-phase sample chambers. Several technological advances are necessary before these conditions are commercially possible. Although wireline pumpout tools may require hours to retrieve representative fluid samples, spending hours obtaining samples in the drilling environment may not be considered a practical alternative. The objective of this thesis is to quantify the viability of sampling in the drilling environment by way of numerical simulations. The study considers the dynamic nature of invasion while drilling when using both new and conventional probe configurations to retrieve fluid samples.

Previous studies assumed a time-constant rate of invasion that was close to that of the final stages of invasion. Furthermore, most simulations of wireline formation-tester measurements assumed that invasion ended at the time when fluid pumpout began. Both of these assumptions are optimistic for a drilling tool. To realistically simulate invasion during drilling, a mudcake model is used that continues to grow in thickness and sealing effectiveness during invasion and throughout the sampling process. Simulation results focus on scenarios in which water-base mud (WBM) and oil-base mud (OBM) invade an oil-bearing zone. In addition, the accuracy of functions used to estimate contamination is studied in an OBM environment. The base model consists of a typical probe-type tool in a vertical well wherein fluid samples are retrieved using a time-constant flow rate. Invasion time is varied from 1 hour to 48 hours to compare drilling and wireline sampling tools. We quantify mudcake sealing effectiveness, as well as the effect of borehole deviation. Oval (elongated) and focusing guard-style probes are compared to standard probe configurations for various petrophysical rock types.

Simulations of fluid cleanup times for a variety of rock types and wellbore deviation angles indicate that the oval focused probe retrieves the cleanest fluid sample in the shortest period of time.

TABLE OF CONTENTS

LIST OF TABLES.....	XI
LIST OF FIGURES.....	XII
CHAPTER 1: INTRODUCTION.....	1
1.1 Introduction.....	1
1.2 Formation-Tester Development.....	2
1.3 Problem Statement.....	3
1.4 Research Objectives.....	4
CHAPTER 2: NUMERICAL SIMULATION OF FORMATION.....	6
2.1 Numerical Simulation.....	6
2.2 Dynamic Mudcake Modeling.....	8
2.3 Validation.....	12
2.4 Petrophysical Assumptions.....	13
CHAPTER 3: SIMULATIONS OF WIRELINE AND WHILE-DRILLING FORMATION-TESTER MEASUREMENTS IN THE PRESENCE OF WBM-FILTRATE INVASION.....	14
3.1 Types of Formation-tester Probes.....	14
3.2 Water-base Mud Modeling.....	16
3.3 Probe Comparison.....	20
3.4 Probe Orientation.....	26
3.5 Probe Behavior For Different Rock-Types.....	28
CHAPTER 4: SIMULATIONS OF WIRELINE AND WHILE-DRILLING FORMATION-TESTER MEASUREMENTS IN THE PRESENCE OF OBM-FILTRATE INVASION.....	30
4.1 Probe Behavior in the presence of obm.....	30
4.2 Oil-Base Mud Contamination Function.....	35
CHAPTER 5: SUMMARY AND CONCLUSIONS.....	41
5.1 Summary.....	41
5.2 Conclusions.....	42

NOMENCLATURE.....	44
REFERENCES.....	45
VITA.....	47

LIST OF TABLES

Table 2.1: Summary of assumed mudcake properties.	10
Table 2.2: Summary of petrophysical properties assumed for four different rock types.	10
Table 3.1: Summary of assumed physical properties of the reservoir.	16
Table 3.2: Summary of assumed fluid properties for the WBM case.	16
Table 3.3: Summary of assumed fluid properties for the WBM case.	17
Table 3.4: Assumed pumpout flow rate for different probes acting on the base-case model.	22
Table 4.1: Equation-of-State parameters and mole fractions of the assumed in situ hydrocarbon pseudo components.	31
Table 4.2: Equation-of-State parameters and mole fractions assumed for the mud-filtrate pseudo components.	31

LIST OF FIGURES

- Figure 2.1:** Simulation of sealing and leaky mud-filtrate invasion. Flow rate and mudcake thickness vary with time. Filtrate loss is negligible at late times and mudcake thickness becomes constant. Although leaky mudcake builds up faster, it entails more filtrate loss than sealing mudcake. 11
- Figure 2.2:** Grid refinement study to appraise simulations of fractional flow and pressure drop. The number of grid blocks increases until simulation results no longer depend on the number of grid blocks. Comparisons are made using simulations of pressure drop both at the start of fluid pumpout and at the time when the probe reaches 5 % of clean oil. ...12
- Figure 2.3:** Saturation-dependent, relative permeability, and capillary pressure for the four synthetic oil-wet rock types described in Table 2.2 (k_{ro} and k_{rw} are oil and water relative permeability, respectively). Relative permeability to oil decreases and capillary pressure increases as permeability and porosity become larger. 13
- Figure 3.1:** Spatial discretization for the numerical simulation of (a) focused sampling, and (b) oval focused probe. Sample probe and guard ring for each probe are defined with point sources within each grid block. Mud-filtrate invasion stops at probe locations during fluid pumpout. 15

Figure 3.2: Contamination, water fractional flow, associated with the four probe-type formation testers for the base-case model. Drawdown begins after 24 hours of WBM invasion. Contamination at the probe is measured as a function of time.18

Figure 3.3: Comparison of pumpout times to investigate the difference between the dynamic mud flow rate, and constant-rate mud-filtrate invasion with sealing mudcake for 10% and 5% of contamination. At short invasion times, the constant-rate invasion model is optimistic, and indicates faster fluid cleanup than dynamic mud-filtrate flow rate. At long high invasion times, the difference between the two becomes smaller than at short invasion times.19

Figure 3.4: Idealized pump performance curve and comparison of single and oval probe performance for the base-case model with a 100 md/cp formation. Drawdown flow rate of probes and resulting pressure drop should both be chosen below the pump curve to operate within the pump’s operational safety margin.21

Figure 3.5: Pressure drop for (a) oval focused probe and (b) focused sampling probe in the base-case model, Rock Type 3, and WBM invasion. The pumpout test begins and the transient pressure drop is recorded after 1 day of mud-filtrate invasion. Increasing the wellbore deviation angle increases the pressure drop during drawdown for types of probes.23

Figure 3.6: Pumpout time for fluid sampling to reach 10% of the contamination level in the presence of WBM invasion, as a function of probe type for the base-case model. (OFP = oval focused probe; FP = focused sampling probe; OP = oval probe; SP = single probe): (a) vertical well, (b) 30-degree deviated well, (c) 60-degree deviated well, and (d) horizontal well. The plots describe the time when each probe reaches 10% of contamination. While-drilling formation testers operate at short invasion times, whereas wireline formation testers operate at long invasion time. The pumpout time necessary to secure a clean fluid sample with wireline formation testers is longer than with while-drilling formation testers.25

Figure 3.7: Magnitude of oil flux at the probe during fluid pumpout. Horizontal slices at the borehole illustrate the difference between oil-flux magnitudes for both focused and the oval focused sampling probes. 26

Figure 3.8: Comparison of simulated cleanup time and pressure drop for focused sampling probe locations along the perimeter of a horizontal wellbore. When the focused sampling probe is located on the side of the well (90-degree orientation from top of the wellbore), cleanup time is faster for short invasion times than when the probe is located at the top of the wellbore (upward position). For the case of pressure drop, there is a lower pressure drop during fluid pumpout when the probe is located to the side of the well than when the probe is located elsewhere. Simulation results were obtained for the base-case model and Rock Type 3, assuming a horizontal/vertical permeability ratio of 10:1.27

Figure 3.9: Assessment of pumpout time for various probes and rock types. The pumpout time necessary to achieve 10% contamination decreases as the permeability and porosity of rock types increase from Rock Type 1 to Rock Type 4. Simulations indicate that the oval focused probe yields the fastest cleanup time for all rock types.29

Figure 4.1: Simulated radial distributions of water saturation and oil density for the cases of invasion with (a) WBM, and (b) OBM for the base-case model. OBM is miscible with in-situ oil, and nearly exhibits a shock radial concentration front. WBM is immiscible and, because of capillary pressure, exhibits a smoother radial saturation front than for the case of OBM-filtrate invasion.....32

Figure 4.2: Comparison of simulated pumpout times for OBM and WBM invasion at an early stage of drawdown when the probes reach 80% of fluid contamination. Results indicate that probes reach 80% of fluid contamination faster in the case of OBM than in the case of WBM.....33

Figure 4.3: Invasion time vs. pumpout time necessary to reach 10% of fluid contamination. For the single probe at short invasion times, there are no significant differences between fluid cleanup times for WBM and OBM contamination. However, at long invasion times (wireline formation tester), significant differences arise between WBM and OBM contamination for the single probe. The oval probe achieves faster cleanup times than the single probe; OBM cleans up more slowly than WBM in this case. Results also show that the probes reach 10% contamination faster in the case of WBM than in the case of OBM.34

Figure 4.4: Comparison of the spatial distributions of WBM and OBM filtrate contamination. The color bar describes oil concentration. At the beginning of pumpout, higher concentrations of oil enter the probe for the OBM case than for the WBM case. However, at the end of the pumpout, WBM exhibits higher contamination than OBM at the probe inlet. Therefore, testers operating in the presence of WBM should obtain a clean fluid sample faster than for the OBM case. ...36

Figure 4.5: Three different contamination functions describe the base-case OBM model. Fluid pumpout begins after 1 hour of mud-filtrate invasion. The GOR contamination function, which is measured at the surface conditions, exhibits a higher level of contamination than the density and viscosity contamination functions, measured at reservoir conditions. There is no indication of decreasing values of contamination with the GOR function, even as pumpout time increases.38

Figure 4.6: Simulated pumpout times for various probe-type formation testers in the presence of (a) WBM-filtrate invasion, and (b) OBM-filtrate invasion (OFP = oval focused probe, FP = focused probe, OP = oval probe, SP = single probe). In the case of WBM-filtrate invasion, probes secure a clean fluid sample faster than in the case of OBM-filtrate invasion. Simulations were performed for the base-case model assuming a reservoir at irreducible water saturation.....40

CHAPTER 1

INTRODUCTION

1.1 INTRODUCTION

Characterization and understanding of reservoir fluid properties is essential throughout the life of a field for effective reservoir evaluation and management. Reservoir fluid studies range from simple fluid tests to full compositional analysis. Well-log data provides initial information on fluid type and productivity. In addition, testing provides confirmation, detailed fluid properties, accurate pressure measurements, and production evaluation.

Formation testing is the final evaluative step before the well is put into production; therefore, it provides essential information. There are common techniques used for formation testing that I will discuss in this thesis. The first one is wireline and while-drilling formation testing. This test uses a probe that can be positioned at a selected depth in the formation to measure fluid pressure and diagnose fluid type. However, the method cannot yield a large sample volume. The second technique uses a packer lowered on drill pipe, wherein the tested interval is not precisely defined and hence the downhole measurement is limited.

Formation testing enables one to measure and/or estimate: (1) formation pressure, (2) permeability, (3) formation skin factor, (4) fluid characterization of reservoir, and (5) perform reservoir characterization.

1.2 FORMATION-TESTER DEVELOPMENT

It has long been realized that sampling fluids and measuring pressure in porous rock formations early in the life of a well provides valuable information about the capability of the formation to produce oil and/or gas. However, this requirement demands for a new generation of formation testers that can reduce both sampling and rig time. Moreover, formation testers are required to secure representative downhole fluid samples, even in complex situations when filtrate is miscible with in-situ reservoir fluid. Industry has introduced optical fluid identification modules for real-time monitoring (Mullins and Schroer, 2000), focused sampling probes (Sherwood, 2005) and, quite recently, the oval pad tester (El Zefzaf et al., 2006). Nonetheless, one of the most important issues about wireline formation sampling remains unsolved, which is acquiring clean reservoir fluid samples with minimum mud-filtrate contamination early in the life of the well.

Although wireline testers are a mature technology, new while-drilling formation testers are emerging, but are currently only designed to measure reservoir pressure (Proett et al., 2003). Even though sampling-while-drilling could be implemented in practice, it is not clear to what extent and how comparable fluid samples would be relative to those acquired with wireline formation testers. It is also not clear what type of formation tester probe should be used to ensure minimally contaminated measurements for a specific tool/formation configuration.

1.3 PROBLEM STATEMENT

Although the effectiveness of fluid sampling in the drilling environment can be simulated, it is important to consider how invasion occurs while drilling. It is pertinent to consider current techniques used for simulation of mud-filtrate invasion. In Previous studies, simulations of fluid cleanup were initialized with a known volume of mud-filtrate invasion (Malik et al., 2009). Other works simulated mud-filtrate invasion before the onset of fluid pumpout, but the invasion rate was stopped after pumpout began (Alpak et al., 2008; Angeles et al., 2009). Both methods are optimistic when analyzing logging-while-drilling (LWD) measurements given that the mudcake is not fully formed at these early stages of drilling and mud-filtrate invasion continues regardless of the test. However, this study does not consider these simplifying assumptions in its intents.

The central objective of this thesis is to compare the following: while-drilling and wireline testers to quantify their effectiveness under different fluid conditions, various petrophysical rock types, and different wellbore deviation angles. These comparisons include simulation results of a recently introduced formation-tester probe geometry. This new formation-tester achieves faster cleanup time with lower pressure differentials imposed on the formation.

To explicitly incorporate the effects of mud-filtrate invasion before and during formation testing, a 3D multi-phase, multi-component reservoir simulator is used that considers gravity and capillary pressure to incorporate the real environment. Mud-filtrate invasion is simulated using a modification of the method proposed by Wu et al. (2004). This method proposes a mathematical model for the dynamic WBM-filtrate invasion. Subsequently, the effects of various contamination functions are investigated to evaluate fluid sample quality with sampling time.

It is also necessary to elaborate on the definition of contamination, which is critical when filtrate is miscible with reservoir fluid. Previous studies proposed to measure gas-oil ratio (GOR) to distinguish the level of contamination of a fluid sample (Alpak et al., 2008). However, there are considerable differences in the assessment of cleanup time when using other types of physical measurements to estimate levels of fluid contamination (e.g. viscosity and density of mud filtrate). Such methods are evaluated to assess contamination against simulations in which contamination is known a priori. In addition, numerical simulations consider the effect of borehole deviation on the performance of various probe configurations.

1.4 RESEARCH OBJECTIVES

The research purposes of the thesis are:

1. To introduce new formation tester probes to acquire clean fluid samples and reduce rig time,
2. To simulate measurements of wireline and while-drilling formation testers in order to assess the effect of water- and oil-base mud filtrate invasion on fluid cleanup time,
3. To introduce a new dynamic mudcake model to describe water- and oil-base mud invasion,
4. To examine the various contamination functions for the case of miscibility between mud-filtrate invasion and reservoir fluid,
5. To assess the effect of borehole deviation on fluid cleanup time,
6. To quantify the efficiency of various probe-type formation testers when operating on various rock types, and

7. To compare the process of fluid cleanup for the processes of oil- and water-base mud-filtrate invasion.

CHAPTER 2

NUMERICAL SIMULATION OF FORMATION

This chapter describes the numerical method used to simulate measurements with probe-type formation testers.

2.1 NUMERICAL SIMULATION

The cases described in this thesis use a multi-phase, multi-component reservoir simulator developed by CMG¹. However, the same method can be applied with other numerical reservoir simulators. In the case of water-base mud (WBM) filtrate invasion, simulations are performed with a black-oil reservoir simulator. In this model, capillary pressure, relative permeability, and other rock-fluid properties, which depend on fluid saturation, are included in the simulations. The model also accounts for the effect of gravity. For simplicity, there is no difference between imbibition and drainage capillary pressure and relative permeability curves during the process of mud invasion and fluid pumpout. A compositional equation-of-state (EOS) simulator is used for oil-base mud (OBM) filtrate invasion and sampling.

To make these simulations more accurate, particularly for formation-tester while-drilling (FTWD), mud invasion must continue during the drawdown or pumpout stages of the simulation. However, mud invasion is prevented from flowing into a selected area of the probe defined as that where the probe creates a seal against the wellbore. Mud invasion continues until the end of the buildup test. The invasion rate can vary throughout

¹ CMG: Computer Modeling Group Ltd.

the entire process and depends on the mudcake model of dynamic filtration described in the next section.

The wellbore boundary is defined by a fine mesh of rectangular grid blocks in the simulation model. Grid blocks adjacent to the wellbore enforce no flow boundary condition; however, mud invasion is simulated by including injection point sources at the grid blocks surrounding the wellbore. This strategy also enables the simulation of invasion-sampling test cases in deviated and horizontal wells.

The type of probe used and its overall dimensions determine how the fundamental base grid blocks are defined. Matching the probe to the simulation grid is a critical step in the modeling given that modeling errors can occur in this region because of high pressure and fluid-concentration gradients. The goal is to construct the grid blocks, so that the number and size result in convergence of the solution. Ideally, when a grid is refined and the solution converges, small variations in the gridding will not affect the result of numerical simulation.

2.2 DYNAMIC MUDCAKE MODELING

The process of modeling dynamic mud-filtrate invasion was first described by Chin (1995) and later used by Wu et al. (2004) to numerically simulate mud-filtrate invasion in deviated wells. This mudcake model was originally developed from first principles by considering the filtration of a fluid suspension of solid particles by a porous but rigid mudcake. It can also be shown that this fundamental model couples mudcake growth to mudcake properties, and formation properties as well as dynamic conditions in annular pressure. A simplified form of the mudcake growth model is given by

$$x_{mc}(t) = \frac{1}{2.54} \sqrt{\frac{2t\Delta P\lambda k_{mc}}{14,696 \mu_m}}, \quad (2.1)$$

where x_{mc} is mudcake thickness (in.), t is time of invasion (sec), k_{mc} is mudcake permeability (md), ΔP is pressure drop across mudcake (psi), μ_m is mud viscosity (cp), and λ is growth factor. As shown in equation 2.1, mudcake thickness depends on the pressure drop across the sandface, and pressure drop depends on the flow rate of mud invasion, which is a function of mud thickness. Flow rate of mud invasion is obtained from

$$q(t) = \frac{2.54 k_{mc} \Delta P}{14,696 \mu_m x_{mc}(t)}, \quad (2.2)$$

where $q(t)$ is mud invasion flow rate ($\text{cm}^3/\text{sec}/\text{cm}^2$). Filtrate viscosity, mudcake permeability, and growth factor are all assumed to remain constant during the invasion process. Flow rate and growth thickness of mudcake are determined with an iterative loop combined with the CMG simulator. Another significant development in this thesis is that

mud-filtrate invasion continues during the pumping or sampling phase. For this reason, samples never reach 0% contamination, as is the case in practical conditions.

In the simulation of WBM and OBM filtrate invasion, both cases assume the same radial length of invasion, time of invasion, and flow rate of invasion. The amount of filtrate loss varies with borehole deviation angle. An increase in wellbore deviation angle increases the volume of mud invasion. Combining the dynamic mudcake modeling directly in the simulation makes it possible to model differences between while-drilling and wireline formation testers. Results would be optimistic if mud-invasion flow rate were considered time-constant throughout the simulation, or the mud-filtrate invasion were stopped during the pumpout test. Table 2.1 summarizes the properties of sealing and leaky mudcake, whereas Table 2.2 illustrates the petrophysical model properties assumed in this thesis.

Figure 2.1 shows the calculated flow rate and thickness of mudcake. The result is in agreement with the experiment that Fisk and Jamison (1989) reported in their work. As shown in Figure 2.1, most filtrate loss typically occurs soon after drilling through the rock and is frequently referred to as spurt or surge loss.

Filtrate loss also depends on the rock type, and varies with the permeability and porosity of the reservoir. In turn, the radius of mud-filtrate invasion also depends on the permeability and porosity of the invaded rock formation.

Table 2.1: Summary of assumed mudcake properties.

Variable	Value	Units
Maximum Thickness	0.1	in
Overbalance Pressure	1000	psi
Filtrate Viscosity	1	cp
Mudcake perm.	0.0001*	md
Growth Factor	0.001**	-

*Sealing mudcake, **Leaky mudcake

Table 2.2: Summary of petrophysical properties assumed for four different rock types.

Rock Type	Horizontal Permeability (md)	Anisotropy (k_v/k_h)	Porosity (fraction)	Irreducible Water Saturation (fraction)
1	1	1	0.1	0.21
2	10	0.1	0.16	0.16
3	100	0.1	0.2	0.11
4	500	1	0.3	0.07

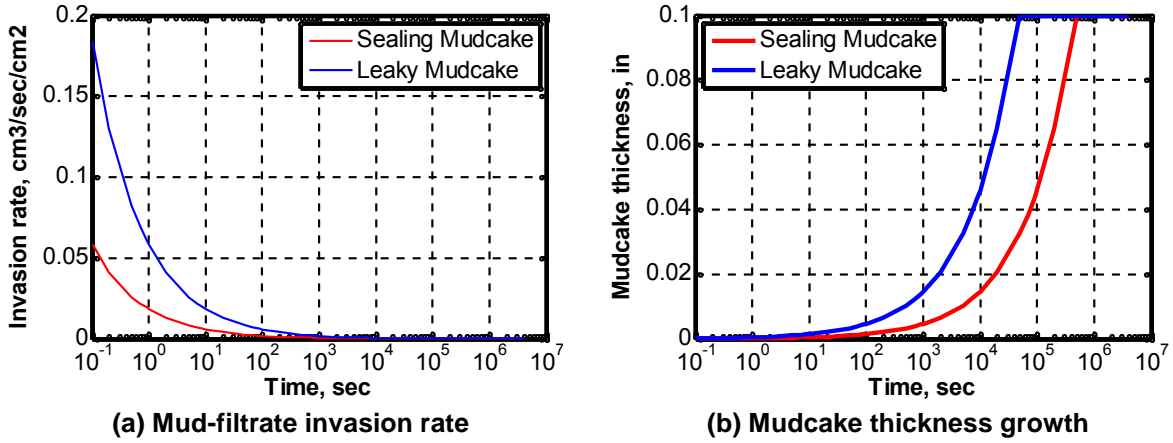


Figure 2.1: Simulation of sealing and leaky mud-filtrate invasion. Flow rate and mudcake thickness vary with time. Filtrate loss is negligible at late times and mudcake thickness becomes constant. Although leaky mudcake builds up faster, it entails more filtrate loss than sealing mudcake.

2.3 VALIDATION

Figure 2.2 shows simulation results obtained from grid refinement studies for the oval and oval focused probe models. For single and focused-sampling probes, the grid mapping used closely matches that used by Angeles et al. (2009). This choice has the advantage of using an established grid in which validations for the numerical discretization and convergence have been previously established. For the new oval and oval focused probes, the size of grid blocks must conform to the size of probe geometry, making it necessary to validate the new gridding strategy. As a result, a base-case model was defined with 317,580 finite-difference grids that constrained the maximum error bounds to less than 0.05% for the simulated values of fractional flow rate and pressure.

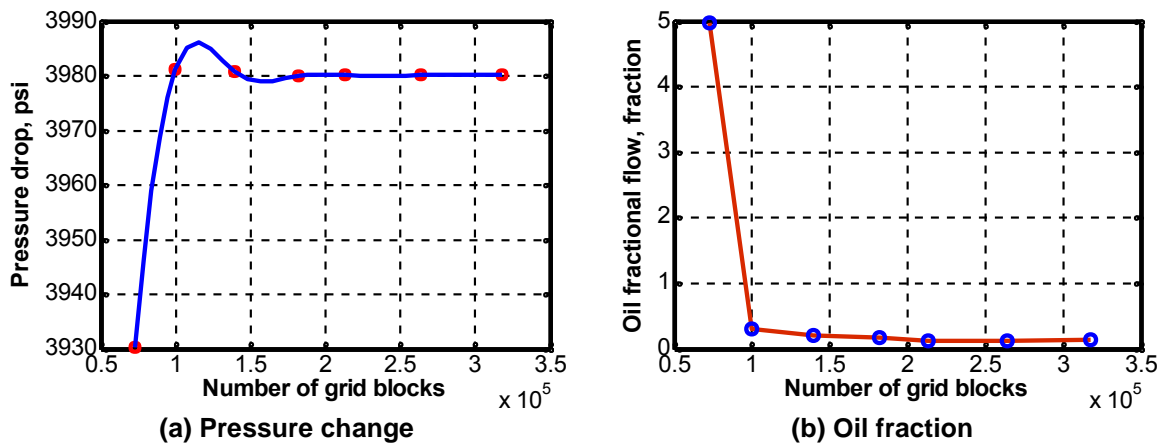


Figure 2.2: Grid refinement study to appraise simulations of fractional flow and pressure drop. The number of grid blocks increases until simulation results no longer depend on the number of grid blocks. Comparisons are made using simulations of pressure drop both at the start of fluid pumpout and at the time when the probe reaches 5 % of clean oil.

2.4 PETROPHYSICAL ASSUMPTIONS

In this study, the base-case model is assumed to be an anisotropic homogenous reservoir. The same capillary pressure and relative permeability curves are used for drainage and imbibition. This simplification was made because previous work showed that such an assumption normally causes very small differences in the simulated pumpout times. Table 2.2 summarizes the assumed rock properties, and Figure 2.3 shows the relative permeability and capillary pressure curves used in the simulations. Rock Type 3, described in Table 2.2, is the base-case model. Synthetic rock types include a wide range of petrophysical properties of reservoirs and are used to evaluate cleanup time for each case of the studied wireline and while-drilling formation testers.

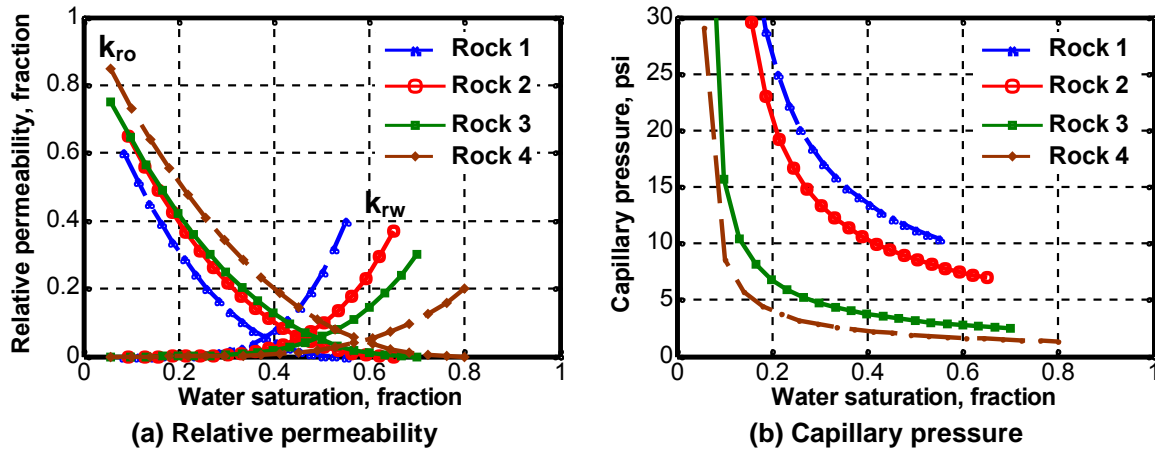


Figure 2.3: Saturation-dependent relative permeability and capillary pressure for the four synthetic oil-wet rock types described in Table 2.2 (k_{ro} and k_{rw} are oil and water relative permeability, respectively). Relative permeability to oil decreases and capillary pressure increases as permeability and porosity increase.

CHAPTER 3

SIMULATIONS OF WIRELINE AND WHILE-DRILLING FORMATION- TESTER MEASUREMENTS IN THE PRESENCE OF WBM-FILTRATE INVASION

This chapter investigates the process of WBM filtrate invasion with different probe-types formation testers. The study also examines the effects of petrophysical properties on contamination cleanup time.

3.1 TYPES OF FORMATION-TESTER PROBES

Four types of probes are considered in the analysis. They include a single probe or conventional probe, an oval pad or elongated oval shape probe, a focused sampling probe, and an oval focused probe. Figure 3.1 shows the configuration of the focused sampling and oval focused probes.

Focused sampling probe and the oval focused probe include two types of probes or flow areas: the sample probe and a guard ring that surrounds the inner sample probe. A sample probe acquires the fluid sample, while the guard ring withdraws contamination fluid surrounding the probe.

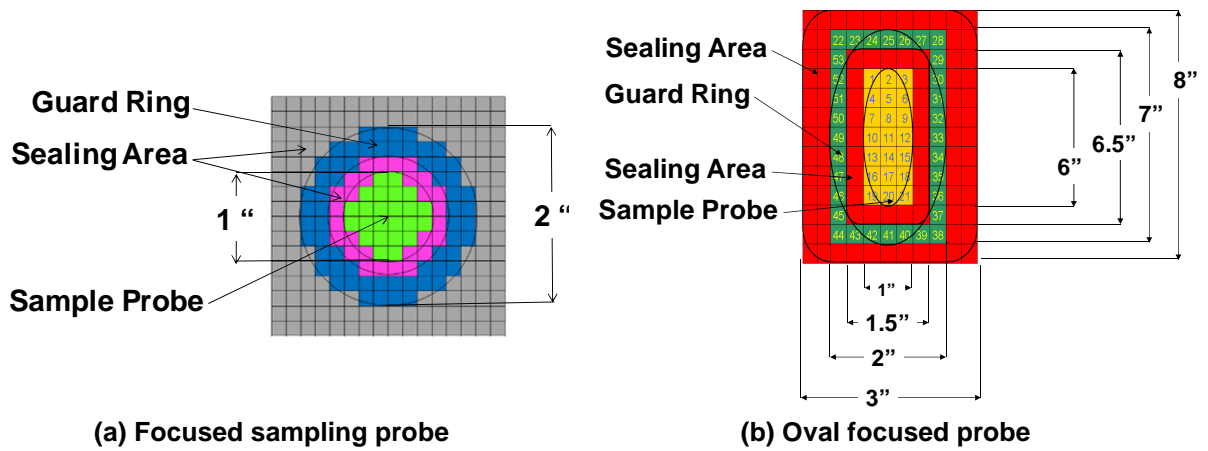


Figure 3.1: Spatial discretization for the numerical simulation of (a) focused sampling, and (b) oval focused probe. Sample probe and guard ring for each probe are defined with point sources within each grid block. Mud-filtrate invasion stops at probe locations during fluid pumpout.

3.2 WATER-BASE MUD MODELING

In the WBM case, a black-oil reservoir simulator is used with the mud-filtrate invasion time varying from 1 to 48 hours. This range includes borehole conditions from while-drilling to wireline formation testers. Tables 3.1 through 3.3 summarize the assumed reservoir, fluid, and PVT properties for the WBM model, respectively.

Table 3.1: Summary of assumed physical properties of the reservoir.

Property	Value	Units
Wellbore Radius	0.354	ft
External Radius	160.0	ft
Reservoir Thickness	30.0	ft
Rock Compressibility	3×10^{-10}	1/psi

Table 3.2: Summary of assumed fluid properties for the WBM case.

Property	Value	Unit
Oil Density	52.4	lbm/ft ³
Water Density	62.4	lbm/ft ³
Oil Compressibility	3×10^{-6}	1/psi
Water Compressibility	2.5×10^{-6}	1/psi
Oil Viscosity	0.5	cp
Water Viscosity	1.0	cp
Oil Bubble Point Press.	500	psi

Table 3.3: Summary of assumed fluid properties for the WBM case.

Pressure	R_s	B_o	B_g	μ_g
psi	scf/STB	RB/STB	cu-ft/scf	cp
14.7	1.0	1.1	6.0	0.008
264.7	90	1.19	82.7	0.009
514.7	180	1.2	159	0.01
1014.7	371	1.21	313	0.014
2014.7	636	1.25	620	0.018
2514.0	775	1.26	773	0.02
3014.7	930	1.28	926	0.022
4014.7	1270	1.31	1233	0.026
5014.7	1600	1.35	1541	0.03
9014.7	2984	1.51	2591	0.047

When pumpout starts, fluid from the reservoir begins to flow into the probe, and mud invasion continues into the formation except at the sealing area of the probes. Cleanup time is measured from the start of the pumpout test. Fractional flow of water to oil entering the probe represents the contamination function for WBM. When the contamination level reaches 5% and 10% of its entire amount, cleanup times or pumpout times are recorded (see Figure 3.2). The contamination function is defined as the fractional flow of water entering the probe in the case of WBM.

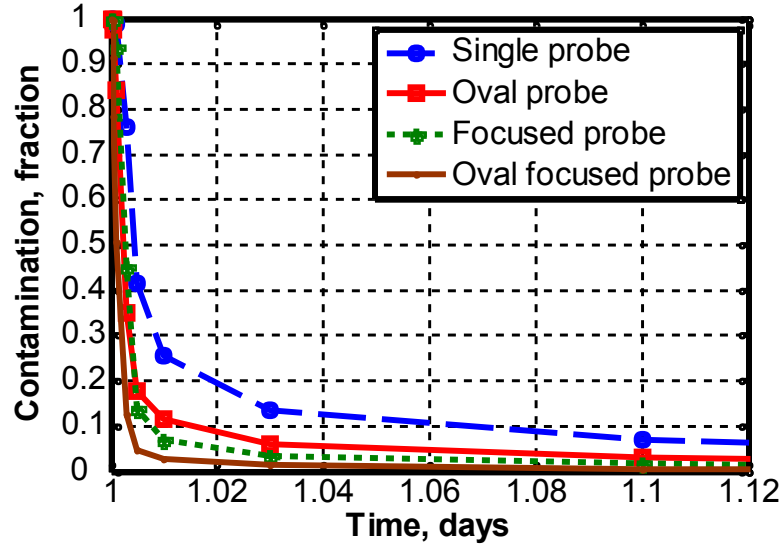


Figure 3.2: Contamination (fractional flow of water) associated with the four probe-type formation testers for the base-case model. Drawdown begins after 24 hours of WBM invasion. Contamination at the probe is measured as a function of time.

Figure 3.3 compares pumpout times calculated for the case of constant-rate mud-filtrate invasion and dynamic mud-filtrate invasion for the four types of probes. For the constant-rate mud invasion case, the rate is determined by averaging the rates for dynamic filtration during the mud invasion period. When comparing the same probe design, the difference between the time-constant invasion rate case and the dynamic invasion case is negligible at long invasion times (i.e. greater than 24 hours). Such a situation arises when mudcake is completely formed for the dynamic case and the total filtrate loss is similar to that of the constant invasion case. These simulation results were obtained using the sealing mudcake properties; results will vary with the assumed mudcake properties.

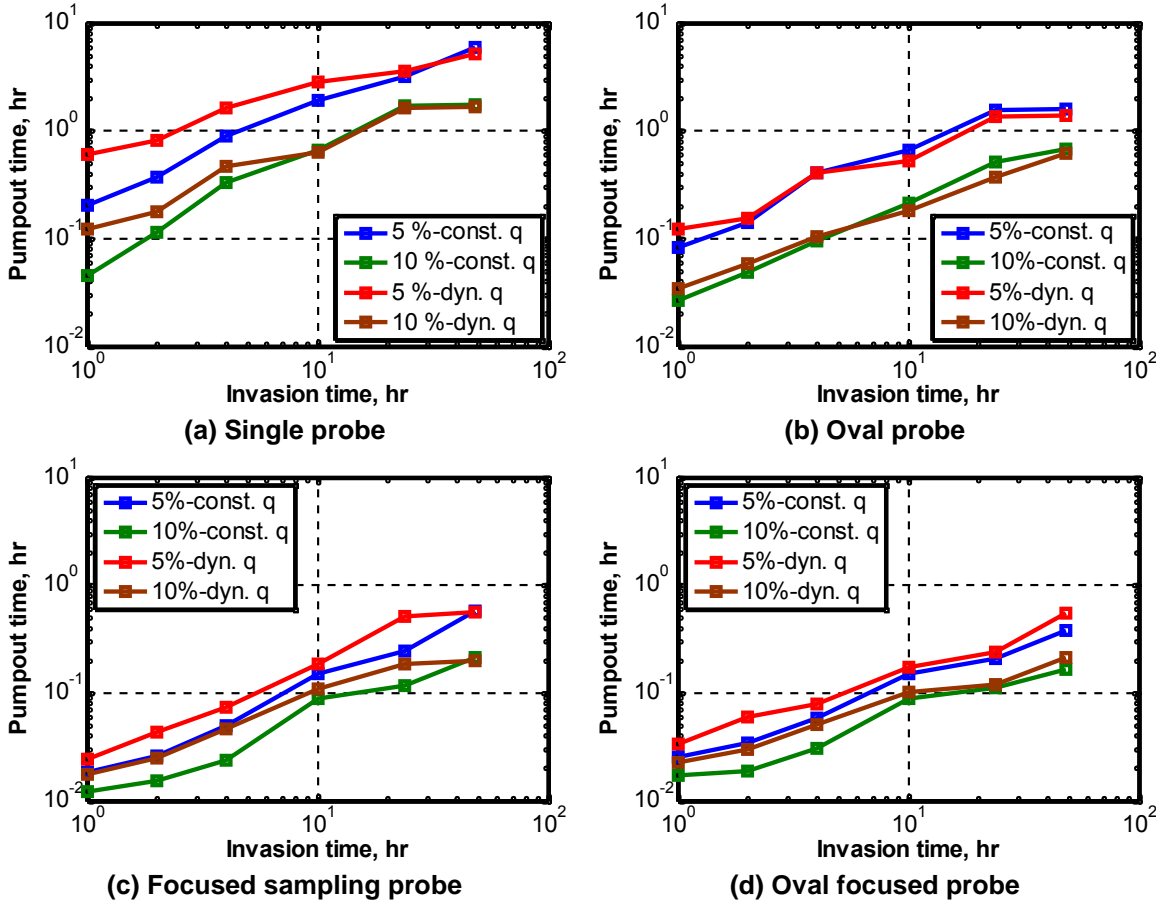


Figure 3.3: Comparison of pumpout times to quantify the difference between both the dynamic mud flow rate, and the constant-rate mud-filtrate invasion with sealing mudcake for 10% and 5% of contamination. At short invasion times, the constant-rate invasion model is optimistic and indicates faster fluid cleanup than dynamic mud-filtrate flow rate. At long high invasion times, the difference between the two becomes smaller than at short invasion times.

3.3 PROBE COMPARISON

When comparing the performance of different probe types, it is necessary to assume a flow rate that is realistic in practical field conditions. The pumpout flow rate of each probe type depends on several factors, namely,

- Probe geometry,
- Available pumping capacity (i.e. pressure vs. rate),
- Reservoir and fluid properties, particularly when it is necessary to maintain the pressure drop for single-phase flow when sampling fluids.

For pumping capacity, we consider the idealized linear pumping curve shown in Figure 3.4. Because the pump must first overcome the overbalance pressure before it can move reservoir fluid, the pump capacity decreases as shown in Figure 3.4. Then the probe geometry, rock type, and fluid properties can be used to generate an idealized linear curve for each probe type, similar to that shown in Figure 3.4, for both single probe and oval probe (El Zefzaf et al., 2006). Therefore, it is only possible to pump at a rate below the threshold point where the probe curve intersects the pump curve. Because both focused sampling and single probe have an equivalent shape and flow area, their pumpout flow rates and pressures are nearly the same. However, as a result of the larger opening of the oval and focused oval probes, they enable greater flow rates than a simple probe at lower pressure differentials under the same conditions (i.e. same pump, rock, and fluid types). While in practical field conditions these curves may not be linear and can shift during pumpout when fluid fractions change, the relative flow rate differences between the two probe types remain the same.

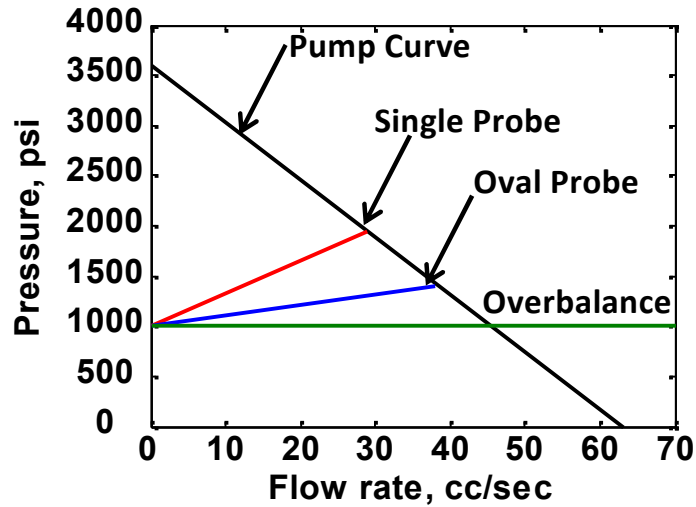


Figure 3.4: Idealized pump performance curve and comparison of single and oval probe performance for the base-case model with a 100 md/cp formation. Drawdown flow rate of probes and resulting pressure drop should both be chosen below the pump curve to operate within the pump’s operational safety margin.

Figure 3.4 shows that for the oval probe, a rate of up to 38 cc/sec is possible for safe operation. To maintain control during pumping, a lower rate is used to remain within the operating margins of the pump. In the base-case simulations, a rate of 30 cc/sec is chosen for the oval and focused oval probes. A rate of 10 cc/sec is used instead to maintain the same differential pressure during pumpout for the single and focused probes. This choice normalizes the flow rates for each probe such that the pressure drop becomes nearly the same during pumpout for all probe types.

Pumpout flow rate of focused and oval focused probes is divided into two flow rates: one for the sample probe and one for the guard ring. The corresponding flow rate of the sample probe to the guard ring can be determined by observing the ratio of rates between the sample and guard ring, which maintains approximately the sample pressure

drop for both regions. As a result, the guard rings operate at a faster flow rate than the sample inner probes. To keep the relative flow rates normalized between the different probe types, the total flow rate for the focusing probes is set equal to the rates used for the unfocused versions. Table 3.4 describes the pumpout flow rate for each probe type in the base-case model reservoir. Although the drawdown flow rate of probes changes across the various rock types, the same analysis is applied to obtain the pumpout flow rates for each probe.

Table 3.4: Assumed pumpout flow rate for different probes acting on the base-case model.

Probe Type	Pumpout flow rate
Single probe	10.0 (cc/sec)
Oval probe	30.0 (cc/sec)
Focused sampling probe	2.5 (cc/sec) Sample probe 7.5 (cc/sec) Guard ring
Oval focused probe	15 (cc/sec) Sample probe 15 (cc/sec) Guard ring

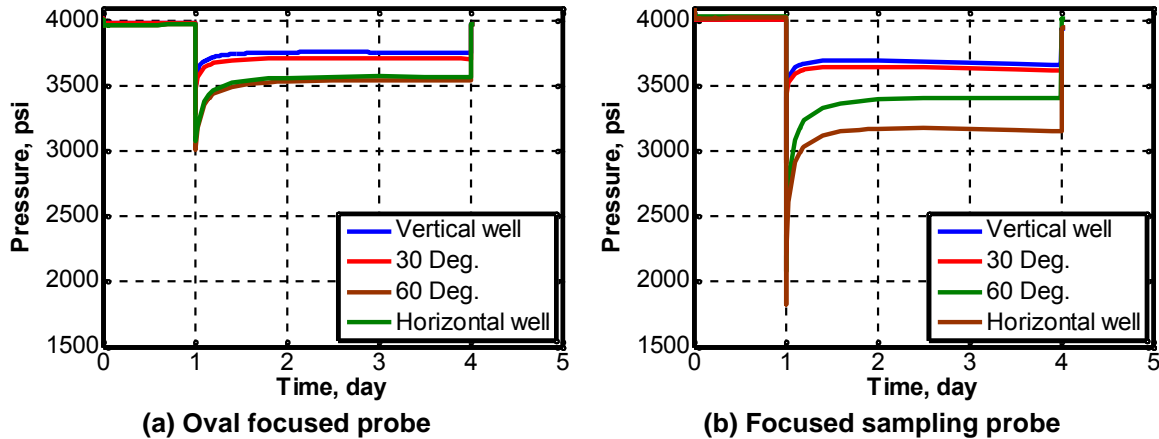


Figure 3.5: Pressure drop for (a) oval focused probe and (b) focused sampling probe in the base-case model, Rock Type 3, and WBM invasion. The pumpout test begins and the transient pressure drop is recorded after 1 day of mud-filtrate invasion. Increasing the wellbore deviation angle increases the pressure drop during drawdown test for all types of probes.

Figure 3.5 describes the simulated pressure drop for oval focused and focused sampling probes as a function of deviation angle for the base-case model, Rock Type 3. Use of the oval probe decreases the pressure drop, especially in highly deviated and horizontal wells.

We use the pumpout time required to reach 10% of WBM contamination to compare the performance of different probes in Figure 3.6. In the case of WBM invasion, water fractional flow defines the contamination function. The four plots in Figure 3.6 show simulations in a vertical well, a 30-degree deviated well, a 60-degree deviated well, and a horizontal well. We observe that increasing the deviation angle increases the pumpout time for all probe types. All plots also show that increasing the invasion time increases pumpout time. This observation indicates that while-drilling formation testers can secure a 10% contaminated sample much faster than a wireline tool. Another

important observation for wireline formation testers is that they are more affected by the deviation of the wellbore than while-drilling formation testers (which work within shorter invasion times). Figure 3.6 also shows that the performance of the probes is consistently ordered with respect to pumpout time from the single, oval, focused, and oval focused probe, which yields the shortest pumpout time. Furthermore, this order is maintained in all base-case simulations when both invasion time and wellbore deviation are varied.

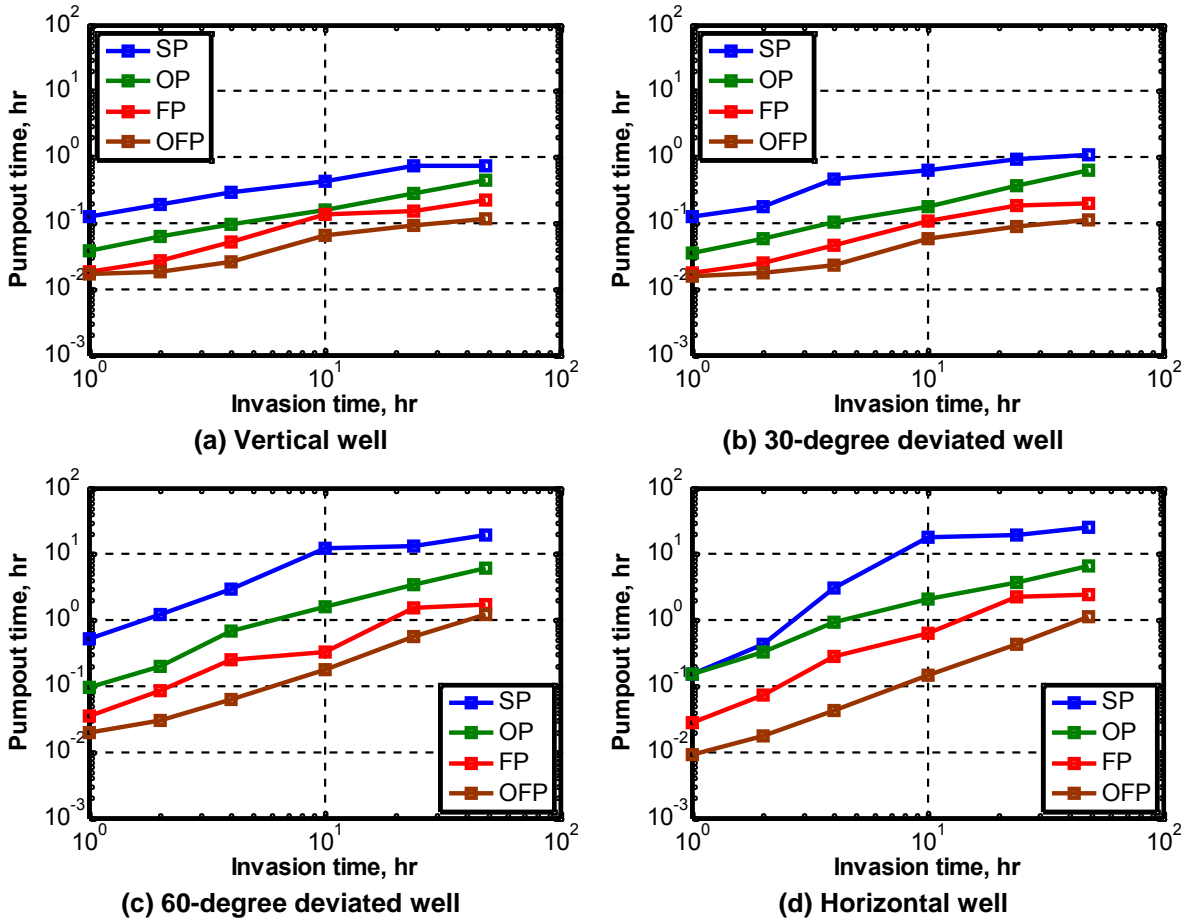


Figure 3.6: Pumpout time for fluid sampling to reach 10% of the contamination level in the presence of WBM invasion, as a function of probe type for the base-case model. (OFP = oval focused probe; FP = focused sampling probe; OP = oval probe; SP = single probe): (a) vertical well, (b) 30-degree deviated well, (c) 60-degree deviated well, and (d) horizontal well. The plots describe the time when each probe reaches 10% of contamination. While-drilling formation testers operate at short invasion times, whereas wireline formation testers operate at long invasion time. The pumpout time necessary to secure a clean fluid sample with wireline formation testers is longer than with while-drilling formation testers.

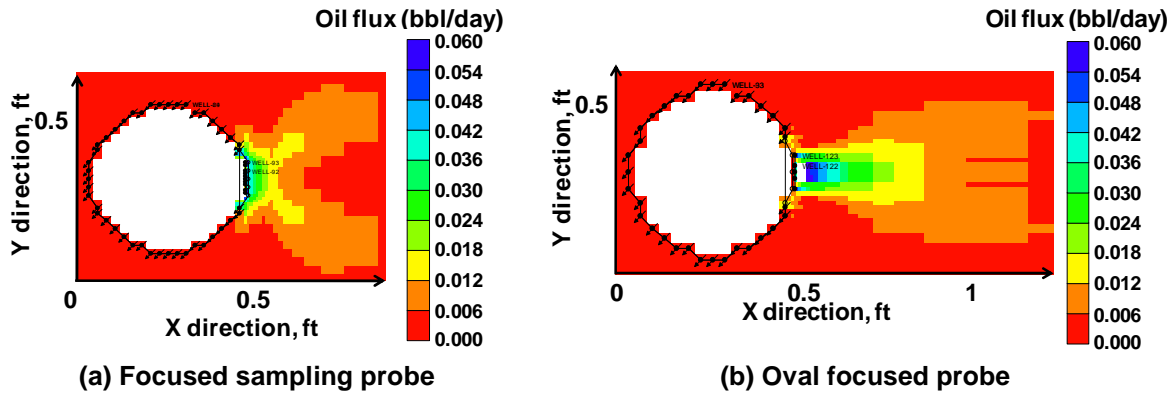


Figure 3.7: Magnitude of oil flux at the probe during fluid pumpout. Horizontal slices at the borehole illustrate the difference between oil-flux magnitudes for both focused and oval focused sampling probes.

3.4 PROBE ORIENTATION

Probe orientation is one of the most important factors affecting fluid cleanup time. The best location for the probe around the perimeter of the wellbore depends on anisotropy, heterogeneity, capillary pressure of the reservoir, and gravity. Gravity tends to drain the invading fluid from the top side of the wellbore, thereby decreasing the volume of contamination to be removed (Angeles et al., 2009). Because of this effect, it is practical to assume that orienting the probe toward the top side of the borehole in deviated wells would reduce pumping time. The studies described in this thesis indicate that for the case of a horizontal well and in the presence of anisotropy (i.e. when horizontal permeability is higher than vertical permeability), the probe should face the upper side of the wellbore (i.e. 90-degree rotation from the top of the wellbore for optimal fluid cleanup time; see Figure 3.8).

Probe orientation becomes more critical in the case of low invasion times encountered with while-drilling formation testers than in the case of wireline testers. For

longer invasion times, the difference in pumpout time for the various probe orientations is not as large.

Figure 3.8 also indicates that when the probe faces the side of the wellbore, pressure drop during pumpout is less than when the probe faces the top of the wellbore. This behavior enables the side-facing probe to pump faster, which further reduces pumpout times.

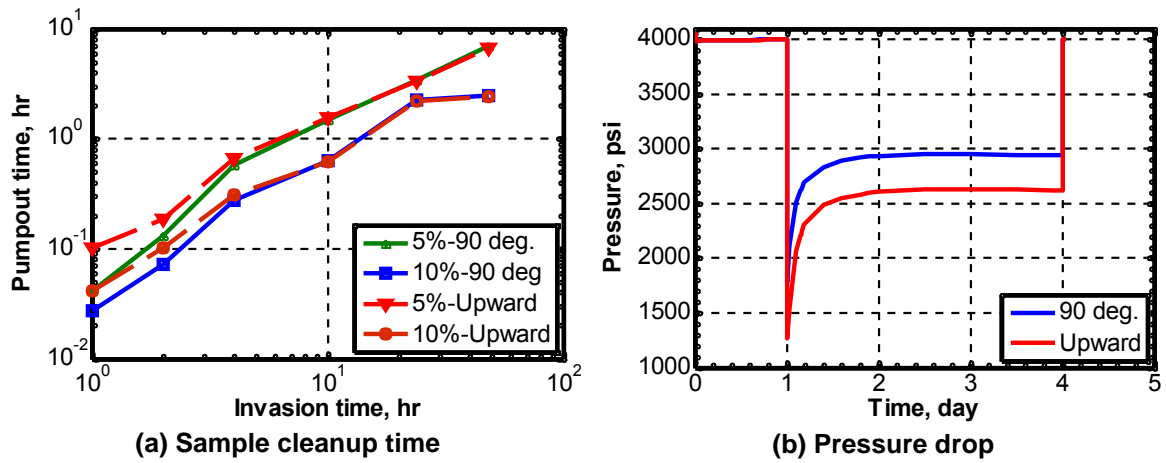


Figure 3.8: Comparison of simulated cleanup time and pressure drop for focused sampling probe locations along the perimeter of a horizontal wellbore. When the focused sampling probe is located on the side of the well (90-degree orientation from top of the wellbore), cleanup time is faster for short invasion times than when the probe is located at the top of the wellbore (upward position). For the case of pressure drop, there is a lower pressure drop during fluid pumpout when the probe is located to the side of the well than when the probe is located elsewhere. Simulation results were obtained for the base-case model and Rock Type 3, assuming a horizontal/vertical permeability ratio of 10:1.

3.5 PROBE BEHAVIOR FOR DIFFERENT ROCK-TYPES

Figure 3.9 describes the behavior of the various probes for four types of rocks. From the pressure drop point of view, the oval and oval focused probes impose a lower pressure drop than the single and focused sampling probes during fluid pumpout.

We emphasize that the radius of mud-filtrate invasion changes with rock type. Although the mud has constant properties, the rock type affects the volume of mud invasion. This observation is confirmed by the behavior of the probes in the four assumed rock types. The pump performance curve, described earlier, determines the flow rate of the pumpout test for each rock type. It also yields the pressure drop for each probe under various reservoir conditions. Simulations for Rock Type 1 show that the single probe cannot achieve 5% contamination. As the rock permeability and porosity increase, the probes achieve a faster cleanup time than in poorer quality rocks.

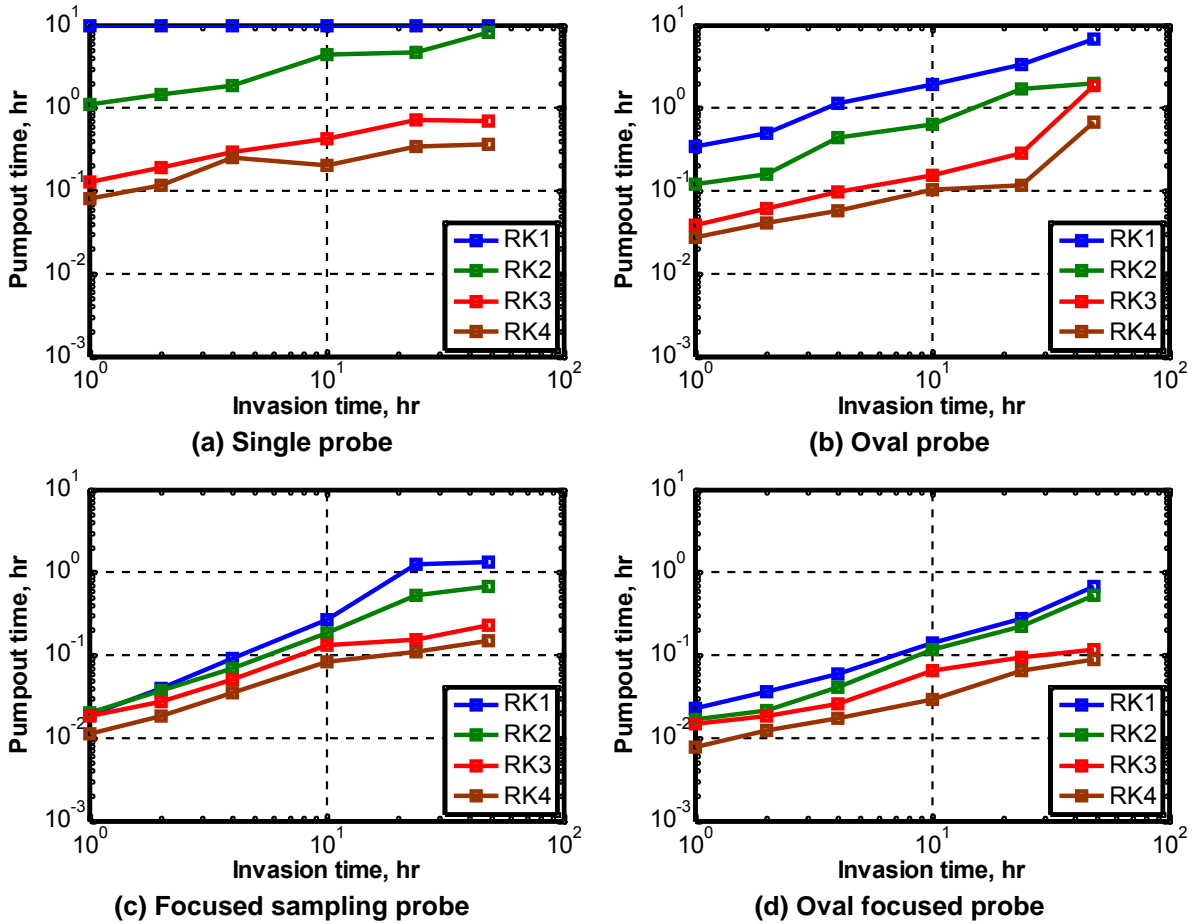


Figure 3.9: Assessment of pumpout time for various probes and rock types. The pumpout time necessary to achieve 10% contamination decreases as the permeability and porosity of rock types increase from Rock Type 1 to Rock Type 4. Simulations indicate that the oval focused probe yields the fastest cleanup time for all rock types.

CHAPTER 4

SIMULATIONS OF WIRELINE AND WHILE-DRILLING FORMATION- TESTER MEASUREMENTS IN THE PRESENCE OF OBM-FILTRATE INVASION

This chapter describes simulation results obtained for the case of OBM-filtrate invasion in a variety of rock types. In addition, we invoke several contamination functions to describe the cleanup procedure in the case of OBM-filtrate invasion.

4.1 PROBE BEHAVIOR IN THE PRESENCE OF OBM

We use the same numerical method to simulate the case of OBM invading an oil-bearing formation, which results in miscible contamination. The reservoir model changes from a black-oil simulator to a compositional equation-of-state (EOS) simulator. In this study, in-situ reservoir fluid and OBM filtrate is tracked using Peng-Robinson's EOS, (Peng and Robinson, 1978). Fluid viscosities are calculated using Lohrenz-Bray-Clark's (LBC) correlation, (Lohrenz et al., 1964), and fluid phase densities are obtained from the EOS.

Tables 4.1 and 4.2 summarize the assumed in-situ oil and OBM properties, together with mole fraction of their components. OBM is heavy, dead oil, and in-situ oil is light oil with a significant amount of soluble gas. OBM filtrate invades the formation with the same volume of filtrate loss as that of WBM. However, because of capillary

pressure, WBM has a smoother radial distribution than OBM. Figure 4.1 shows the differences in the contamination front with water and OBM invasion at increasing radial distances from the wellbore.

Table 4.1: Equation-of-State parameters and mole fractions of the assumed in situ hydrocarbon pseudo components.

Parameter	N ₂ C ₁	CO ₂ -C ₃	C ₄ -C ₆	C ₇ -C ₁₈	C ₁₉₊
Molar concent.	0.6	0.07	0.08	0.1	0.03
Critical temp. (°F)	-126	125	359	656	1060
Critical press. (psi)	653	839	498	322	184
Acentric factor	0.01	0.14	0.2	0.4	0.9
Molecular weight (lbs/mole)	16	36	67	132	303
Volume shift parameter	-0.1	-0.13	-0.05	0.17	0.23

Table 4.2: Equation-of-State parameters and mole fractions assumed for the mud-filtrate pseudo components.

Parameter	MC ₁₄	MC ₁₆	MC ₁₈
Molar concentration	0.6	0.2	0.1
Critical temperature (°F)	755	822	878
Critical pressure (psi)	261	240	224
Acentric factor	0.6	0.7	0.7
Molecular weight (lbs/mole)	190	222	251
Volume shift parameter	0.07	0.06	0.04

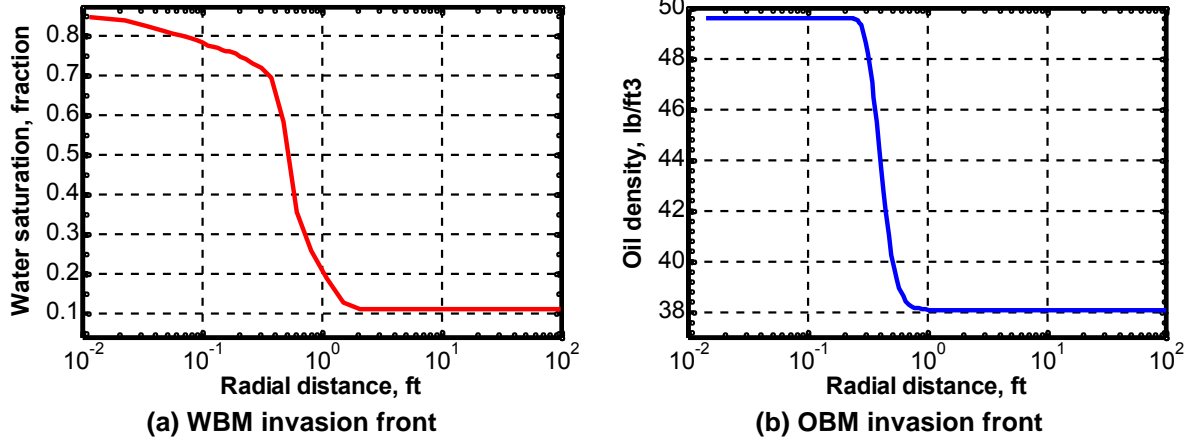


Figure 4.1: Simulated radial distributions of water saturation and oil density for the cases of invasion with (a) WBM, and (b) OBM for the base-case model. OBM is miscible with in-situ oil, and nearly exhibits a shock radial concentration front. WBM is immiscible and, because of capillary pressure, exhibits a smoother radial saturation front than for the case of OBM-filtrate invasion.

As a result of capillary-pressure effects, simulations indicate that WBM spreads more than OBM in the radial distance, and that OBM results in a more piston-like radial front of invasion.

For the base-case model, Rock Type 3, assumed at irreducible water saturation, it takes longer for OBM to clean up and reach 10% of contamination than with WBM. However, OBM contamination cleans up faster than WBM contamination at the beginning of the pumpout test. As shown in Figure 4.2, OBM reaches 80% contamination faster than WBM.

Because WBM and OBM have the same viscosity, which is higher than that of in-situ reservoir oil, both create an invaded zone with lower formation mobility than the uncontaminated regions. However, WBM invasion is immiscible, which results in a much lower invaded-zone mobility than with OBM. For the case of WBM, the contaminated

region is governed by immiscible mixing, which further reduces formation mobility in the contaminated region as a result of relative permeability effects.

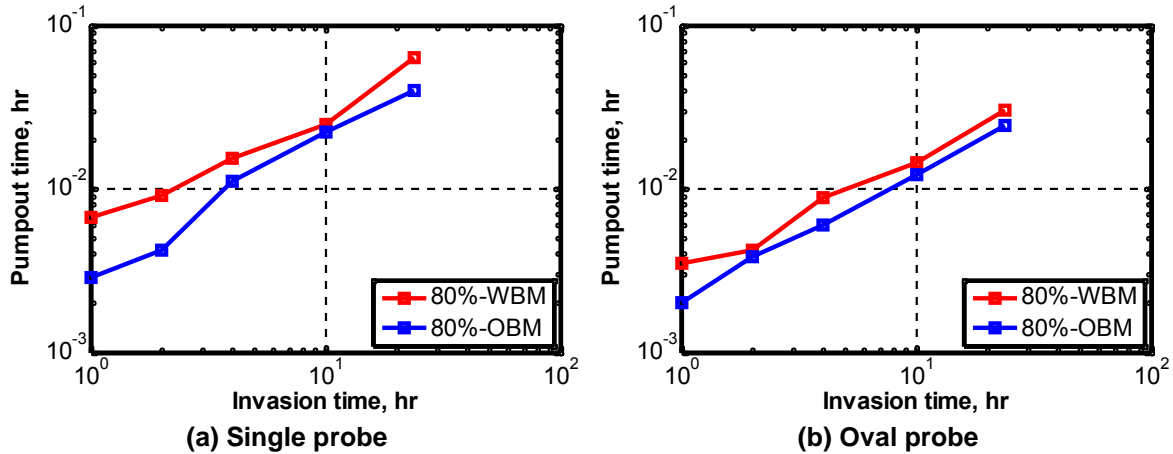


Figure 4.2: Comparison of simulated pumpout times for OBM and WBM invasion at an early stage of drawdown when the probes reach 80% of fluid contamination. Results indicate that probes reach 80% of fluid contamination faster in the case of OBM than in the case of WBM.

During pumpout, a channel forms to funnel the in-situ oil to the probe. Because of the lower viscosity of native oil, the channel has lower formation mobility than the invaded region. For the case of WBM, the creation of this channel is slower because of the reduced formation mobility of the invaded region, as compared to the case of OBM. Therefore, after the start of the pumpout test, in the case of OBM, the probes withdraw contamination and create a channel more quickly than with WBM.

However, as pumpout continues a more focused channel ensues because the lower formation mobility (WBM-invasion region) acts as a guard to the oil that has penetrated a path to the probe. This path, or channel, has higher formation mobility because of the reduced contamination (i.e. lower water saturation) than the surrounding WBM-invaded

region. In the OBM case, the created channel also has lower formation mobility than the surrounding invaded region, but the contrast is much lower. Consequently, OBM filtrate is more mobile and mixes more freely with the oil present in the flow channel path to the probe, thereby resulting in a slower cleanup time for the WBM case. This conclusion is best shown in Figures 4.2 and 4.3, which compare simulated pumpout times for the single and the oval probes using the base-case WBM and OBM models. Both simulation results assume the same radius of mud-filtrate invasion shown previously in Figure 4.1.

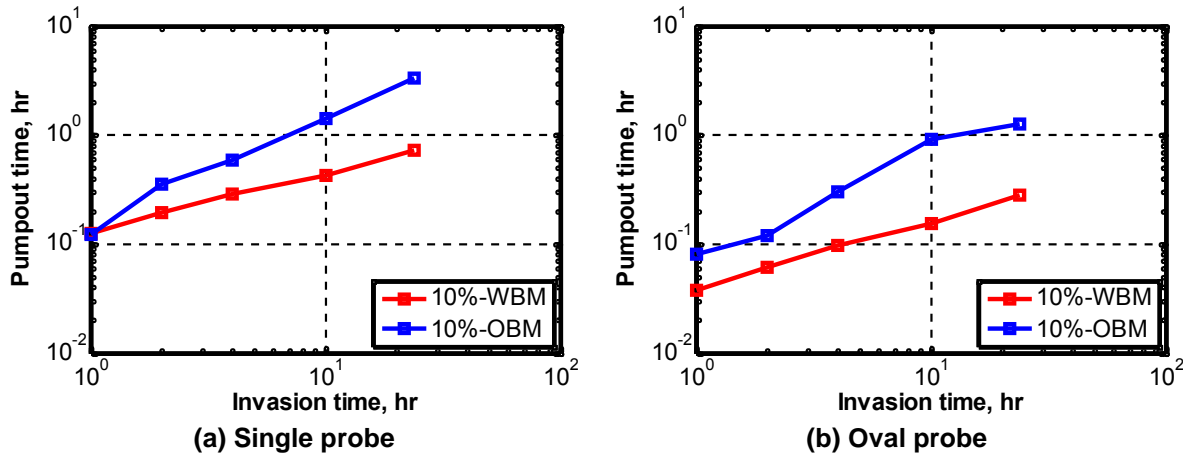


Figure 4.3: Invasion time vs. pumpout time necessary to reach 10% of fluid contamination. There are no significant differences between fluid cleanup times for WBM and OBM contamination for the single probe at short invasion times. However, at long invasion times (wireline formation tester), significant differences arise between WBM and OBM contamination for the single probe. The oval probe achieves faster cleanup times than the single probe; OBM cleans up more slowly than WBM in this case. Results also show that the probes reach 10% contamination faster in the case of WBM than in the case of OBM.

Figure 4.4 describes the invaded flow channel pattern by showing the concentration contrast in the flow channel at the beginning and end of a pumpout test. The region surrounding the channel behaves as a non-ideal insulator, which performs

better with WBM than with OBM. Consequently, lower contamination leaks into the channel with WBM than with OBM, and yielding shorter sampling times with WBM.

4.2 OIL-BASE MUD CONTAMINATION FUNCTION

Estimating the contamination with a miscible mud filtrate poses some difficulties because filtrate and in-situ oil (or water) can have similar properties. There are currently several methods to estimate contamination and evaluate pumpout times for OBM. These contamination functions are based on volumetric measurements of contamination, such as gas-oil ratio (GOR), or molar-base measurements, including fluid density and viscosity.

Because GOR is normally measured at the surface, a downhole measurement of GOR would not be a direct measurement and would be subject to correlation errors. In turn, correlation errors can result in discrepancies in the GOR downhole estimate when compared to the surface measurement. Downhole GOR can also be misleading if gas is produced while sampling because the sampling vessel may not retain both phases effectively. In addition, GOR is not directly related to the volume fraction of the contamination.

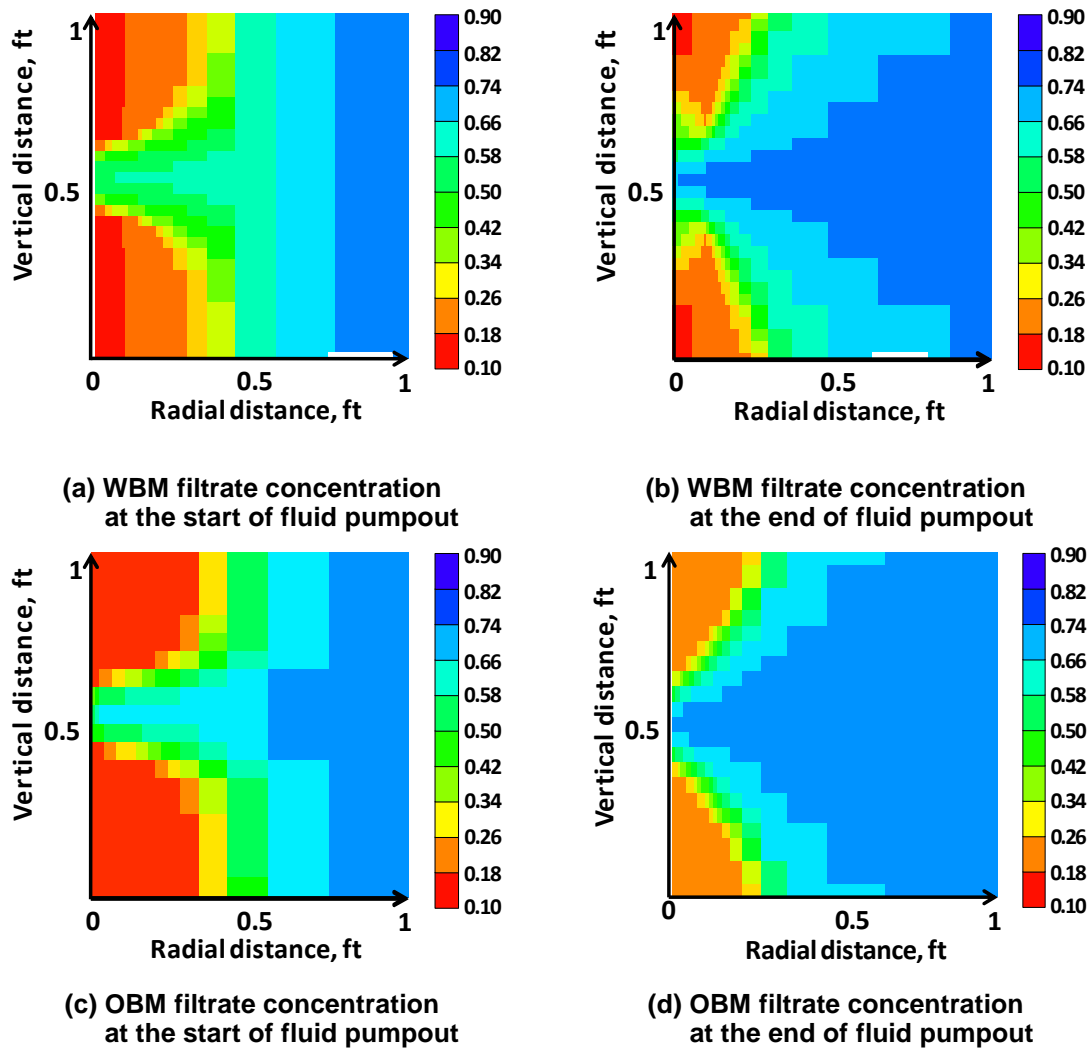


Figure 4.4: Comparison of the spatial distributions of WBM and OBM filtrate contamination. The color bar describes oil concentration. At the beginning of pumpout, higher concentrations of oil enter the probe for the OBM case than for the WBM case. However, at the end of the pumpout, WBM exhibits higher contamination than OBM at the probe inlet. Therefore, testers operating in the presence of WBM should obtain a clean fluid sample faster than for the OBM case.

Austad and Isom (2001) introduced the GOR-based contamination function given by

$$C(t) = 1 - \frac{1}{\frac{\rho_m}{\rho_o} \left\{ \frac{GOR_o}{GOR(t)} - 1 \right\} + 1}, \quad (3.1)$$

where $C(t)$ is contamination as a function of sampling time, t is time, ρ_m is mud density, ρ_o is in-situ oil density, GOR_o is uncontaminated formation GOR, and $GOR(t)$ is measured GOR.

The corresponding contamination function based on density is given by

$$C(t) = \frac{\rho(t) - \rho_o}{\rho_m - \rho_o}, \quad (3.2)$$

where $\rho(t)$ is measured density, ρ_o is formation oil density, and ρ_m is mud density.

For the case of viscosity, the contamination function is given by

$$C(t) = \frac{\mu(t) - \mu_o}{\mu_m - \mu_o}, \quad (3.3)$$

where $\mu(t)$ is measured viscosity, μ_o is formation oil viscosity, and μ_m is mud viscosity.

This contamination function assumes that viscosity mixing is linear between the fluid

phases involved; however, it can be modified to include non-linear mixing rules, such as Todd and Longstaff's (1972) or the modified Arrhenius model (Lederer, 1933).

As shown in Figure 4.5, the GOR contamination estimate consistently indicates a higher level of contamination than molar-based contamination functions. The density function should be the most accurate because density mixes linearly and the exact densities in the simulations are known a priori. However, in practice, when filtrate and formation fluid densities are similar, the accuracy decreases.

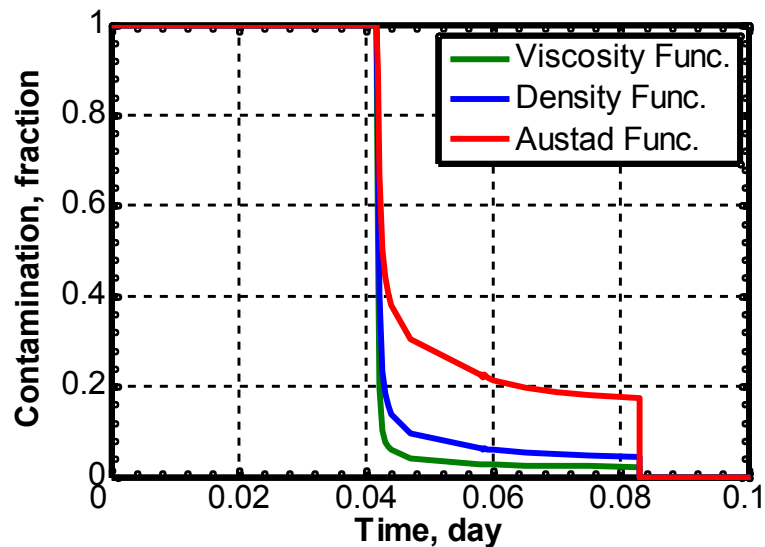


Figure 4.5: Three different contamination functions describe the base-case OBM model. Fluid pumpout begins after 1 hour of mud-filtrate invasion. The GOR contamination function, which is measured at surface conditions, exhibits a higher level of contamination than the density and viscosity contamination functions, measured at reservoir conditions. There is no indication of decreasing values of contamination with the GOR function, even as pumpout time increases.

Based on the density contamination function, we calculate cleanup time for OBM in the base-case model and for the four types of probes shown in Figure 4.6. For the cases of focused sampling and oval focused probes, results exhibit the same trend because the shapes of these probes are similar to the single and oval probes, respectively. For the case of the single probe, the difference in cleanup time between OBM and WBM becomes significant when invasion times are large, which occurs with wireline formation testers. For the oval probe, a difference exists between cleanup time for small and large invasion times. As indicated by the simulation results shown in Figure 4.6, the oval probe cleans up faster than the single probe in both OBM and WBM cases. For the single and focused sampling probes, there is little difference between cleanup times for cases of OBM and WBM invasion when invasion times are short (i.e. 1 to 2 hours). For short invasion times, Figure 4.6 indicates that oval-type probes clean up faster in the case of WBM invasion. In the OBM base case, the single probe requires significantly longer cleanup times to produce clean fluid than the remaining probes.

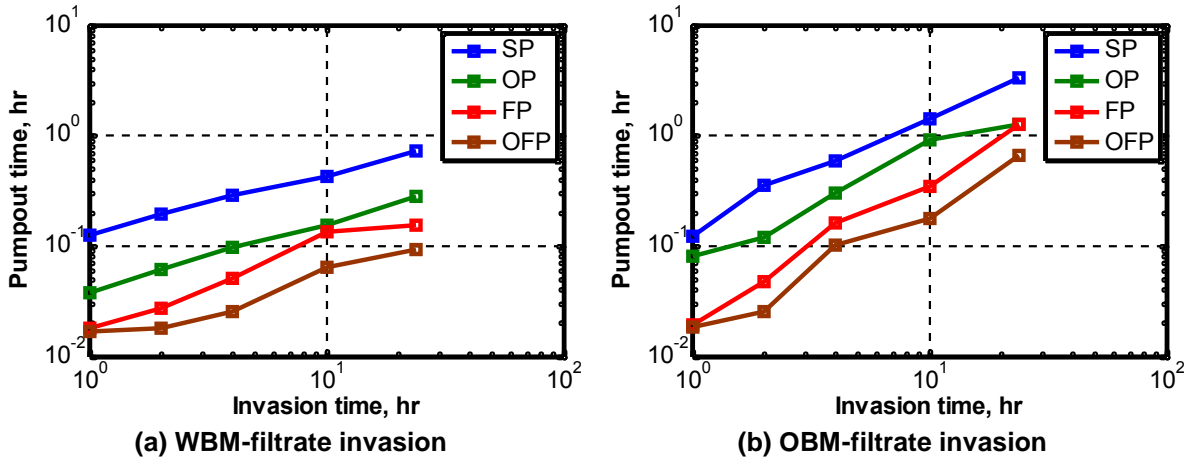


Figure 4.6: Simulated pumpout times for various probe-type formation testers in the presence of (a) WBM-filtrate invasion, and (b) OBM-filtrate invasion (OFP = oval focused probe, FP = focused probe, OP = oval probe, SP = single probe). In the case of WBM-filtrate invasion, the probes secure a clean fluid sample faster than in the case of OBM-filtrate invasion. Simulations were performed for the base-case model assuming a reservoir at irreducible water saturation.

CHAPTER 5

SUMMARY AND CONCLUSIONS

5.1 SUMMARY

A notable improvement of this thesis, with respect to previous related studies, is the explicit consideration of dynamic mud-filtrate invasion during fluid pumpout. This was a feature of the simulations because one of the primary goals was to compare the performance of wireline testers to that of while-drilling testers. The study shows that formation testers can secure clean fluid samples soon after drilling much faster than wireline testers under the same conditions. Each probe investigated in this thesis was associated with its own performance curve. By considering the available pump and sampling constraints (i.e. saturation pressure), one can choose the appropriate probe for a specific rock type. Changes in formation mobility near the probe were considered in the analysis because the change of near-wellbore mobility affects the pressure drop and is an important practical consideration to control pumpout.

The density contamination function is based on a molar-based measurement of contamination, and provides an improved estimate of contamination compared to the commonly used GOR contamination estimates. Although the GOR method is considered a volume-base estimate, it yields a consistently higher contamination level compared to the value that can be determined directly from measured simulations.

When comparing OBM and WBM simulations, OBM models are associated with faster clean up times than WBM models at the beginning of the pumpout test. However, for testers to acquire low-level contamination samples (i.e. less than 10%), a WBM system is normally faster than OBM regardless of probe design.

5.2 CONCLUSIONS

The following conclusions stem from the numerical simulations and interpretation studies considered in this thesis:

1. While-drilling formation testers are typically associated with shorter pumpout times than wireline formation testers, even when considering active invasion while sampling.
2. Based on simulations of different probe designs under a variety of reservoir conditions, the oval focused probe retrieves the cleanest fluid sample in the shortest time, followed by the standard focused probe, the oval probe, and, finally, by the single probe.
3. The largest simulated pressure drop during fluid pumpout corresponds to the single probe, followed by the oval probe, focused sampling probe, and, finally, the oval focused probe.
4. Pumpout cleanup time increases with wellbore deviation angle regardless of probe type. The effect of wellbore deviation on increasing cleanup times is the largest for the single probe, followed by the oval probe, focused sampling probe, and the oval focused probe.
5. The pressure drop during pumpout increases with wellbore deviation angle. This behavior may lead to abnormal two-phase flow in the near-borehole region.

6. At irreducible water-saturation conditions and for the same invasion radius, cleanup times are faster for WBM-filtrate invasion than OBM-filtrate invasion.
7. Molar-based contamination functions are more reliable and accurate than volumetric functions, such as GOR, to quantify the time evolution of fluid cleanup.
8. Because of formation anisotropy, capillary pressure, fluid density contrast, and wellbore deviation angle, it is recommended that probes face the upper side of the wellbore when operating in a horizontal well to achieve the shortest fluid cleanup time and to operate at the lowest possible pressure drop during pumpout.
9. Fluid pumpout time increases with decreasing quality of petrophysical properties (i.e. lower permeability, lower porosity, and higher capillary pressure). For the simulation cases considered in this thesis, the oval focused or focused sampling probes consistently achieved the fastest cleanup times.

NOMENCLATURE

λ	: Growth factor
$C(t)$: Time-dependent contamination
ΔP	: Pressure drop across mudcake, [psi]
$x_{mc}(t)$: Mudcake thickness, [in]
k_{mc}	: Mudcake permeability, [mD]
$q(t)$: Flow rate of mud-filtrate invasion, [cm ³ /sec/cm ²]
ρ_m	: Mud density, [lb/ft ³]
ρ_o	: In-situ oil density, [lb/ft ³]
μ_m	: Mud viscosity, [cp]
μ_o	: Formation oil viscosity, [cp]
μ_g	: Formation gas viscosity, [cp]
R_s	: Solution gas oil ratio, [scf/STB]
B_g	: Gas formation volume factor, [ft ³ /STB]
B_o	: Oil formation volume factor, [RB/STB]
ϕ	: Porosity
k	: Formation permeability, [mD]
k_{rw}	: Water relative permeability
k_{ro}	: Oil relative permeability
GOR	: Gas-oil ratio, [ft ³ /STB]
GOR _o	: Uncontaminated formation GOR, [ft ³ /STB]
GOR(t)	: Measured GOR, [ft ³ /STB]
OFP	: Oval focused probe
FP	: Focused sampling probe
OP	: Oval probe
SP	: Single probe
S _{wirr}	: Irreducible water saturation
OBM	: Oil-base mud
WBM	: Water-base mud
EOS	: Equation-of-state
FTWD	: Formation tester while-drilling
LWD	: Logging-while-drilling

REFERENCES

- Alpak, O.F., Elshahawi, H., Hashem, M., and Mullins, O., 2008, Compositional Modeling of Oil-Based-Mud-Filtrate Cleanup during Wireline Formation Tester Sampling, *SPE Reservoir Evaluation and Engineering*, v. 11, no. 2, April, p. 219-232.
- Angeles, R., Torres-Verdín, C., and Malik, M., 2009, Prediction of Formation-Tester Fluid-Sample Quality in Highly Deviated Wells, *Petrophysics*, v. 50, no. 1, February, p. 32-48.
- Austad, T. and Isom, T.P., 2001, Compositional and PVT Properties of Reservoir Fluids Contaminated by Drilling Fluid Filtrate, *Petroleum Science and Engineering*, v. 30, p. 213-244.
- Chin, W.C., 1995, *Formation Invasion, with Applications to Measurement While Drilling, Time Lapse Analysis and Formation Damage*, Gulf Publishing Company, Houston, Texas.
- El Zefzaf, T., El Fattah, M.A., Proett, M., Engelman, B., and Bassiouny, A., 2006, Formation Testing and Sampling Using an Oval Pad in Al Hamed Field, Egypt, paper SPE 102366 presented at the SPE Annual Technical Conference and Exhibition, San Antonio, Texas, USA, 24-27 September.
- Fisk, J.V. and Jamison, D.E., 1989, Physical Properties of Drilling Fluids at High Temperature and Pressures, *SPE Drilling Engineering*, v. 4, no. 4, December, p. 341-346.
- Lederer, E. L., 1933, Mixtures: On Reducing Viscosity, *Proc. World Petroleum Congress*, v. 2, p. 526-528.
- Lohrenz, J., Bray, B.G., and Clark, C.R., 1964, Calculating Viscosity of Reservoir Fluids from Their Compositions, *Journal of Petroleum Technology*, v. 16, no. 10, October, p. 1171-1176.
- Malik, M., Torres-Verdín, C., and Sepehrnoori, K., 2009, A Dual-Grid Automatic History Matching Technique with Applications to 3D Formation Testing in the Presence of Oil-Base Mud, *SPE Journal*, v. 14, no. 1, March, p. 164-181.
- Mullins, O.C. and Schroer, J., 2000, Real-Time Determination of Filtrate Contamination During Openhole Wireline Sampling by Optical Spectroscopy, paper SPE 63071 presented at the SPE Annual Technical Conference and Exhibition, Dallas, Texas, 1-4 October.

- Peng, D.Y. and Robinson, D.B., 1976, A New Two-Constant Equation-Of-State, *Industrial and Engineering Chemistry Fundamentals*, v. 15, no. 59, p. 59-64.
- Proett, M., Walker, M., Welshans, D., and Gray, C., 2003, Formation Testing While Drilling, A New Era in Formation Testing, paper SPE 84087 presented at the SPE Annual Technical Conference and Exhibition, Denver, Colorado, USA, 5-8 October.
- Sherwood, J.D, 2005, Optimal Probes for Withdrawal of Uncontaminated Fluid Samples, *Physics of Fluids*, v. 17, issue 8, p. 83102/1-83102/10.
- Todd, M.R. and Longstaff, W.J., 1972, The Development, Testing and Application of a Numerical Simulator for Predicting Miscible Flood Performance, *Journal of Petroleum Technology*, v. 24, no. 7, July, p. 874-882.
- Wu, J., Torres-Verdín, C., Sepehrnoori, and K., Delshad, M., 2004, Numerical Simulation of Mud-Filtrate Invasion in Deviated Wells, *SPE Reservoir Evaluation and Engineering*, v. 7, no. 2, April, p. 143-154.